Research Article

Kamalesh Balakumar Venkatesan, Saravanan Alamelu, Sivamathi Rathna Priya, Nivedha Jayaseelan, Sathish-Kumar Kamaraj, Manoj Kumar Srinivasan*, Mohammed Ali Alshehri, Chellasamy Panneerselvam*, Ahmed Saif, and Selvendiran Periyasamy

Ameliorated antimicrobial, antioxidant, and anticancer properties by *Plectranthus vettiveroides* root extract-mediated green synthesis of chitosan nanoparticles

https://doi.org/10.1515/gps-2023-0086
received May 27, 2023; accepted September 4, 2023

Abstract: In this investigation, using the biogenic approach, *Plectranthus vettiveroides* root extract was used to synthesize chitosan nanoparticles (*P. vettiveroides* CNPs). The produced nanoparticles (NPs) were characterized using UV-visible (UV/vis) absorption spectroscopy, Fourier transform infrared (FTIR) spectroscopy, and scanning electron microscopy (SEM). The typical absorption peaks in the UV/vis spectra were located around 253 nm. Functional groups were identified in *P. vettiveroides* CNPs by FTIR. As per SEM analysis, the NPs generated exhibited a spherical shape with an average diameter of 78.01 nm. In addition, the synthesized *P. vettiveroides* CNPs were examined for antioxidant and antibacterial properties and anticancer activities. They show a strong antioxidant activity compared to butylated hydroxytoluene as a standard antioxidant. *P. vettiveroides* root extract CNPs demonstrated the most significant zone of inhibition against *Klebsiella pneumoniae* (22 mm), followed by *Escherichia coli* (21 mm), *Bacillus cereus* (19 mm), and *Staphylococcus aureus* (17 mm). In addition, using MTT assay, anticancer efficacy against KB (oral cancer) cells was studied. The cytotoxic reaction was observed in a dosage-dependent manner. *P. vettiveroides* CNPs show bioefficacy because of their size and the existence of bioactive compounds, which can enhance antibacterial and anticancer activities by lysing bacterial and cancer cell walls.

Keywords: antibacterial, anticancer, antioxidant, chitosan nanoparticles, *Plectranthus vettiveroides*

*** Corresponding author: Manoj Kumar Srinivasan,** Department of Biochemistry and Biotechnology, Faculty of Science, Annamalai University, Chidambaram, India, e-mail: manojsrinivasan1002@gmail.com
*** Corresponding author: Chellasamy Panneerselvam,** Department of Biology, Faculty of Science, University of Tabuk, Tabuk, Saudi Arabia, e-mail: cpselva@ymail.com
Kamalesh Balakumar Venkatesan, Saravanan Alamelu, Sivamathi Rathna Priya, Nivedha Jayaseelan: Department of Biochemistry and Biotechnology, Faculty of Science, Annamalai University, Chidambaram, India
Sathish-Kumar Kamaraj: Instituto Politécnico Nacional (IPN)-Centro de Investigación en Ciencia Aplicada y Tecnología Avanzada, Unidad Altamira (CICATA-Altamira), Carretera Tampico-Puerto Industrial Altamira Km 14.5, C. Manzano, Industrial Altamira, 89600 Altamira, Tamps, Mexico
Mohammed Ali Alshehri: Department of Biology, Faculty of Science, University of Tabuk, Tabuk, Saudi Arabia
Ahmed Saif: Department of Clinical Laboratory Sciences, Central Research Laboratory, College of Applied Medical Science, King Khalid University, Abha 61321, Saudi Arabia
Selvendiran Periyasamy: Environmental and Water Resources Division, Department of Civil Engineering, Indian Institute of Technology Madras, Chennai, Tamil Nadu 600 036, India

Abbreviation

$ABTS^{\bullet+}$	2, 2′-Azinobis-(3-ethylbenzothiazoline-6-sulfonic acid)
BHT	Butylated hydroxytoluene
CNPs	Chitosan nanoparticles
DMEM	Dulbecco's modified Eagle's medium
DMRT	Duncan's multiple range tests
DMSO	Dimethyl sulfoxide
DPPH	1,1-Diphenyl-2-picryl hydroxyl
FBS	Fetal bovine serum
FRAP	Ferric reducing antioxidant power
FTIR	Fourier transform infrared spectroscopy
H_2O_2	Hydrogen peroxide
MTT	3-(4,5-Dimethylthiazol-2-yl)-2,5-diphenyltetrazolium bromide

NCCS	National Centre for Cell Sciences
NPs	Nanoparticles
O_2–	Superoxide anion
SEM	Scanning electron microscopy
TCA	Trichloroacetic acid
TPP	Sodium tripolyphosphate

1 Introduction

Chitosan is a naturally occurring poly-cation deacetylated polymer made of *D*- and *N*-acetyl glucosamine groups. Chitosan comes in various molecular weights, has intriguing properties, and can be used in various industrial processes, most notably for medication delivery. Chitosan particles could be created as nanoparticles (NPs), microspheres, and microcapsules. Chitosan, via its amino groups, will engage in a wide range of chemical processes [1]. Natural polymers are superior to synthetic polymers mainly because they are biodegradable, non-toxic, and biocompatible [2]. NPs are tiny (1–100 nm) chemical compounds with functional unity. These substances have the potential to be used as medicinal substances, transfection vectors, antibacterial agents, and fluorescent labels, and their use in consumer goods and medical applications is growing [3]. Root extract-based biogenic nanoscale metal particles are becoming increasingly important. Since using biological sources to synthesize trustworthy, eco-friendly nanoscale materials, bio-nanotechnology is an intriguing and developing technical instrument. Chitosan nanoparticles (CNPs) used now include food packaging, gene therapy, heavy metal removal, reducing agent metal NP medication delivery systems, and antibacterial activities [4]. CNPs aid water purification by adsorbing pollutants, while biomedically they enable drug delivery and wound healing. Additionally, chitosan supports catalysis and green chemical processes through functionalized NPs [5]. Numerous conventional techniques have been used to create NPs, but these techniques have several drawbacks, including cost, the production of toxic chemicals, and others. As a result, research has been intensified to develop safe, ecologically acceptable alternatives for generating NPs, emphasizing biological systems as a primary green method. From an industrial and commercialization standpoint, large-scale synthesis of CNPs using green sources like plants is practical to a certain extent. Advantages include the sustainability of plant-based sources, reduced environmental impact, and potential cost savings. However, drawbacks may include variability in chitosan content among different plant species, slower extraction processes, and potential scalability challenges. Additionally, ensuring consistent quality and yield may pose challenges, warranting further optimization for reliable and efficient production [6]. Biological systems can create exact forms and manage structures [7]. The ionic gelation approach has garnered much interest among the techniques developed to make CNPs since it is non-toxic, devoid of organic solvents, practical, and controlled. The ion gelation method is commonly used to form NPs from chitosan. This process involves the crosslinking of chitosan molecules to create stable NPs through the use of ions, such as tripolyphosphate (TPP), which act as crosslinking agents [8,9]. The root extract of *Plectranthus vettiveroides*, which contains negatively charged groups, was used in this study to create CNPs instead of other artificially negatively charged materials. This novel process is based on the ionic gelation technique. *P. vettiveroides* is a fragrant, herbaceous plant member of the *Lamiaceae* family. Locally, it is known as Lavanchi and Muchivala in Kannada, Vettiveru and Kuriver in Telugu, Vetiver and Kuru ver in Tamil, Valak in Hindi, and Iruveli in Malayalam [10]. Its lamina is relatively thin, its roots are fragrant, and its leaves are unscented. Additionally, the extract of *P. vettiveroides* exhibits antimicrobial, antifungal, and antioxidant activities. Glycosides, phenolic content, terpenoids, anthraquinones, saponin, tannins, and lignin were found in the methanol extracts of *P. vettiveroides*, using the phytochemical analysis. The root extract biomolecules may serve as catalysts for the biosynthesis of CNPs. This system has a few intriguing characteristics: (a) a biological system; very gentle circumstances; and no use of high temperature, surfactant, or other specialized experimental technologies are required to create the NPs and (b) because of their small size and positive surface charges, NPs may be more stable in bioactivities by engaging with negatively charged biomembranes and being linked to specific areas *in vivo* [11]. Biomolecules present in plant extracts have the potential to be used in the manufacture of NPs. However, many chemicals in aromatic and therapeutic plants are biologically active. On the other hand, as far as we know, *P. vettiveroides* aqueous root extracts have never been used to manufacture CNPs. So, for the first time, this work investigates the synthesis of CNPs using *P. vettiveroides* root extracts and their antibacterial, antioxidant, and anticancer activities.

2 Materials and methods

2.1 Reagents

Sodium phosphate, sodium carbonate, potassium acetate, chloroform, methanol, ethyl acetate, sulfuric acid, ethylenediaminetetraacetic acid, hydrogen peroxide (H_2O_2), and

trichloroacetic acid reagents were purchased from Qualigens (Mumbai). 3-(4,5-Dimethylthiazol-2-yl)-2,5-diphenyltetrazolium bromide (MTT), chitosan, sodium TPP, 1,1-diphenyl-2-picryl hydroxyl (DPPH), and butylated hydroxytoluene (BHT) were purchased from Sigma Aldrich. All other substances used in this study were of the highest quality and analytical grade. KB (oral cancer) cells were procured from NCCS (National Centre for Cell Sciences), Pune, India.

2.2 Collection of plant material and plant extract

Root samples of the plant *P. vettiveroides* were collected from Kodumudi Dam, Cuddalore district, Chidambaram, Tamil Nadu. A Botanist at the Department of Botany, Annamalai University, identified the collected plant material.

P. vettiveroides root extract was prepared from collected roots. About 10 g of the finely chopped root was used and boiled for 5 min in 100 ml of ethanol. The resulting extract was cooled and filtered using Whatman No. 1 filter paper and kept at 4°C for storage.

2.3 Synthesis of CNPs

CNPs were made using a modified version of the previously described ionic gelation of chitosan with TPP anions [12]. 20 mg of chitosan were mixed with 20 ml of 1% (V/V) acetum (acetic acid) solution at room temperature under continuous magnetic stirring. Subsequently, the pH was adjusted to 5.5. Next, 3.5 ml of 2.0 $mg{\cdot}ml^{-1}$ TPP was dropwise added to the chitosan solution. Transient sonication resulted in the formation of an opaque and transparent solution. By pouring 1 ml of *P. vettiveroides* ethanol solution with a concentration of 3 $mg{\cdot}ml^{-1}$ into the chitosan solution before adding TPP, *P. vettiveroides*-loaded CNPs (*P. vettiveroides* CNPs) were synthesized (Figure 1). After centrifuging the NPs at 8,000 rpm, 4°C for 30 min, collecting the supernatant, and suspending the precipitate after three double distilled water washes, the NPs were lyophilized.

The synthesized CNPs were subjected to various characterization techniques to determine their unique characteristics. A UV-visible (UV/vis) spectrometer was used to record the absorption spectrum for optical qualities, and an scanning electron microscopy (SEM) was used to assess the form of CNPs.

2.4 Antibacterial activity

Antimicrobials and antibiotics are substances that eradicate bacterial growth. It is only possible to use novel molecules not derived from synthetic antimicrobial drugs to prevent antibiotic resistance [13]. In this study, the antibacterial effects of *P. vettiveroides* CNPs have been examined on the bacterial strains *Escherichia coli, Staphylococcus aureus, Bacillus cereus,* and *Klebsiella pneumoniae*. Ampicillin is used as the standard antibiotic treatment for particular bacterial species. On a plate of solidified agar, the pure solvent was inoculated with microorganisms in a 1:1 ratio for the control experiment.

2.5 Antioxidant activity

2.5.1 $DPPH^{\bullet}$ antioxidant assay

The antioxidant activity of the *P. vettiveroides* CNPs against $DPPH^{\bullet}$ was measured using the method described in Brand Williams et al.'s study [14]. The stable free radical DPPH can accept hydrogen radicals (H) or an electron to create a stable molecule. When it mixes with a free radical that may produce H, DPPH is reduced. It was documented when the hue changed (from deep violet to blue). *P. vettiveroides* CNPs in various concentrations totaling 1 ml were introduced with 1 ml of DPPH and 3 ml of water. The produced blue color was read at 517 nm using BHT as a reference.

$$\text{DPPH antioxidant activity (\%)} = (A1 - A2)/A1 \times 100$$

The absorbance of the control is $A1$, whereas the absorbance of the sample is $A2$.

2.5.2 $ABTS^{\bullet+}$ (2, 2′-azinobis-(3-ethylbenzothiazoline-6-sulfonic acid)) assay

Using the method described in Re et al.'s study, the $ABTS^{\bullet+}$ radical cation decolorization test was used to measure the total free radical activity of samples [15]. As was already discussed, the inhibition% was calculated.

2.5.3 Ferric reducing antioxidant power (FRAP) assay

Benzie and Strain developed the FRAP method, which can determine the antioxidant capability of *P. vettiveroides* CNPs [16]. This approach intends to transform a ferric tripyridyltriazine complex into its ferrous-colored version in the presence of antioxidants.

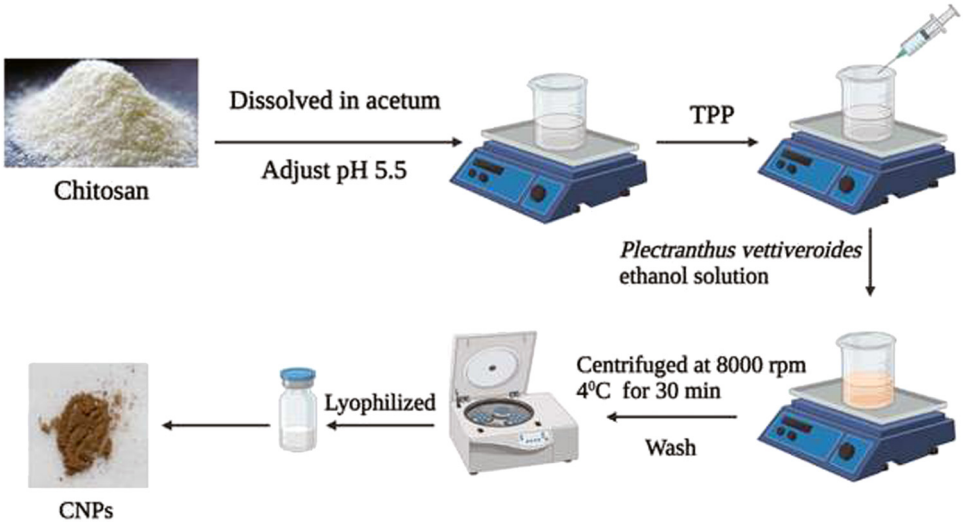

Figure 1: Synthesis of *P. vettiveroides* CNPs.

2.5.4 $O2^{\bullet-}$ (superoxide anion) assay

Liu et al. calculated the superoxide anion scavenging activity [17]. About 0.1 ml of *P. vettiveroides* CNPs (25–100 μg^{-1}) was added to 1 ml of nitro blue tetrazolium chloride (NBT), reduced nicotinamide adenine dinucleotide, and other chemicals. At 25°C, this mixture was incubated for a few minutes. The reagent mixture was used as a control, but no sample was added. The absorbance was spectrophotometrically determined at 560 nm. BHT was used as a reference standard. The percentage of inhibition was determined.

2.5.5 H_2O_2

Using the Nebavi et al.'s method, the *P. vettiveroides* CNPs capacity to scavenge H_2O_2 was assessed [18]. About 1.2 ml of H_2O_2 and 2.0 ml of *P. vettiveroides* CNPs (25–100 µg) in phosphate buffer (pH 7.4) were added. A blank tube was created using the same method but without including H_2O_2. The absorbance at 230 nm was calculated following 10 min of incubation. The percentage of inhibition was estimated using BHT as the reference standard.

2.6 MTT (cytotoxicity assay)

The KB cells were cultured in Dulbecco's modified Eagle's medium (DMEM), media with 10% FBS (fetal bovine serum), and 1% antibiotics (penicillin–streptomycin) in 5% CO_2 incubator at 37°C. The MTT test was used to assess the cytotoxicity of the *P. vettiveroides* CNPs.

To get the KB cells to adhere to the plates, they were seeded in a 96-well plate at a density of 5×10^{-3} cells per well and then incubated for around 24 h. After washing away the culture medium, the cells were treated with *P. vettiveroides* CNPs diluted in DMEM at 25, 50, 75, 100, and 125 $\mu g \cdot ml^{-1}$ concentrations. A separate group of untreated cells was kept in identical circumstances as the treated cells. After 24 h of incubation, 20 µl of MTT solution was added to each well, followed by an additional 4 h of 37°C incubation.

The mitochondria of living cells react with the MTT reagent to produce a purple formazan. The media were removed from each well, and 100 µl of dimethyl sulfoxide (DMSO) was used to dissolve the formazan crystals. The absorbance at 570 nm was determined using a microplate reader [19]. The % cell viability was estimated as follows:

$$\% \text{ Cytotoxicity} = 100 - \% \text{ Cell viability}$$

2.7 Statistical analysis

All the biochemical assays were carried out in triplicate. The mean and standard deviation were used to present experimental test results. One-way analysis of variance was used to analyze the data using SPSS version 21, and DMRT (Duncan's multiple range tests) was used to compare the group averages.

3 Results and discussion

3.1 Analytical characterization

3.1.1 UV/vis spectroscopy

The primary applications of UV/vis spectroscopy are the identification and qualitative evaluation of chemical compounds. The presence of absorption peaks at 253 nm in the UV/vis spectra suggests the occurrence of electronic transitions within *P. vettiveroides* CNPs (Figure 2). These transitions relate to the material's molecular structure and conjugation, providing insights into its optical and electronic properties, aiding in characterizing and understanding the composition and behavior Of NPs.

3.1.2 Fourier transform infrared (FTIR) analysis

Figure 3 shows the FTIR spectra of CNPs *P. vettiveroides*. FTIR analysis confirms the involvement of these phytochemicals by revealing characteristic peaks at 3,448, 2,810, 1,674, 1,467, 1,124, and 619 cm^{-1} corresponding to O–H, C–H bond, NH^{3+}, −COO, C═O, and C–O functional groups, indicative of their binding to the NPs. This dual function of phytochemicals in the synthesis of CNPs underscores their significance in promoting eco-friendly and efficient NP production.

3.1.3 SEM

SEM was used to examine the surface morphology of *P. vettiveroides* root extract CNPs (Figure 4). The SEM findings demonstrated the existence of NP aggregates and spherical shapes with excellent resolution. The SEM images were used to produce a particle size distribution histogram, which revealed significant variance in the particle size. The diameters of the particles range from 10 to 140 nm, with a mean and standard deviation of 78.01 and 23.67 nm, respectively (Figure 5).

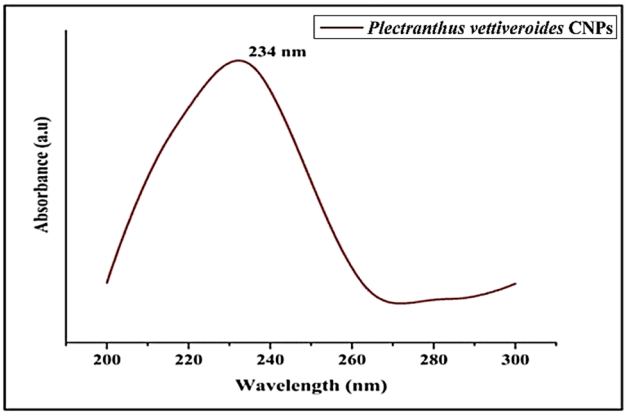

Figure 2: UV/vis spectroscopy of CNPs synthesized using *P. vettiveroides* root extract.

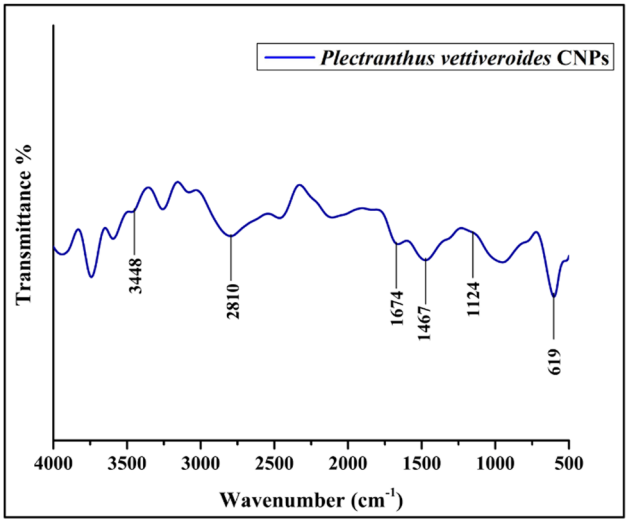

Figure 3: FTIR spectrum CNPs synthesized using *P. vettiveroides* root extract.

3.2 Antibacterial activity

A reliable diffusion technique was used to evaluate the antibacterial activity of *P. vettiveroides* CNPs against

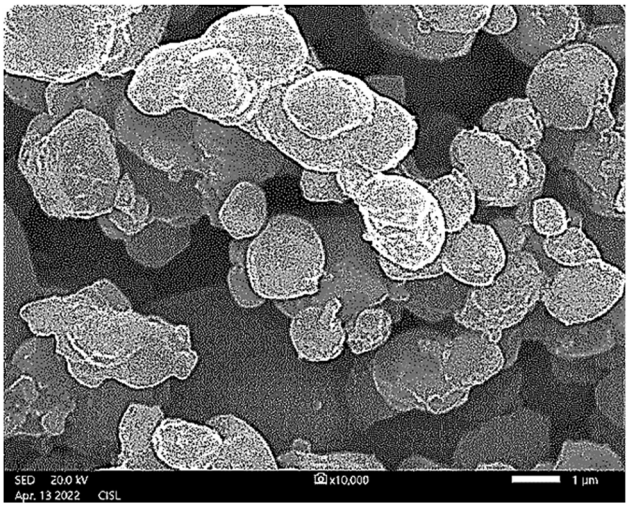

Figure 4: SEM image of CNPs synthesized using *P. vettiveroides* root extract.

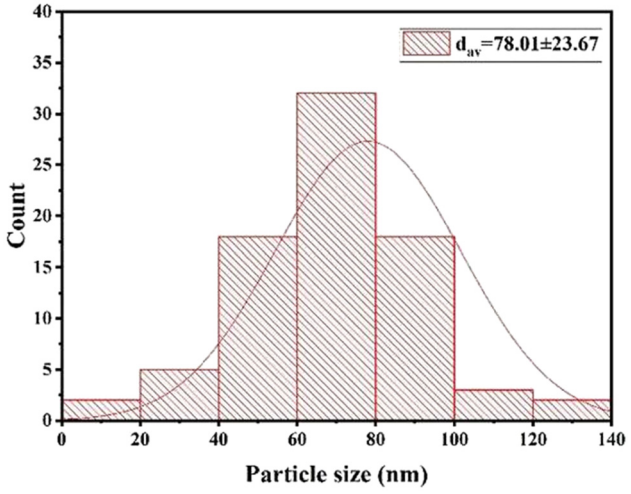

Figure 5: SEM image of CNPs synthesized using *P. vettiveroides* root extract determined using a particle size distribution histogram.

bacterial pathogens (*S. aureus, B. cereus, E. coli,* and *K. pneumoniae*). The results are given in Figures 6 and 7 and Table 1. The biosynthesized CNPs demonstrated an antibacterial activity on all the studied bacterial strains. Based on the differences in the structural makeup of Gram-positive (+ve) and Gram-negative (−ve) bacteria, the bactericidal impact of CNPs was determined to be stronger for −ve bacteria than for +ve bacteria. At 100 µg concentrations, *P. vettiveroides* root extract CNPs demonstrated the most significant zone of inhibition against *K. pneumoniae* (22 mm), followed by *E. coli* (21 mm), *B. cereus* (19 mm), and *S. aureus* (17 mm).

3.3 Antioxidant activity

3.3.1 Effect of *P. vettiveroides* CNPs on DPPH radical scavenging activity

Our results show that the *P. vettiveroides* CNPs have a similar free radical scavenger activity as BHT (Figure 8). It was evident that the *P. vettiveroides* CNPs showed proton-donating activities, indicating that they may be used as free radical scavengers or inhibitors even though their extreme scavenging capacities of DPPH were somewhat inferior to those of BHT. The *P. vettiveroides* CNPs suppressed the DPPH radical by 36.62%, 39.21%, 45.25%, and 49.91% at 25, 50, 75, and 100 µg·ml^{-1}, respectively. The findings of this study suggest that the ability of *P. vettiveroides* CNPs to donate hydrogen may serve as primary antioxidants, which in turn mediates their capacity to scavenge free radicals.

3.3.2 Effect of *P. vettiveroides* CNPs on ABTS radical scavenging activity

Synthesized *P. vettiveroides* CNPs nearly matched the standard BHT in their ability to neutralize $ABTS^{\bullet+}$ (Figure 9). The percentage of inhibition for *P. vettiveroides* CNPs was 47.13% at 100 µg·ml^{-1} concentration.

3.3.3 Effect of *P. vettiveroides* CNPs on FRAP radical scavenging activity

The present findings showed that *P. vettiveroides* CNPs and BHT have a dose-dependent reducing power, ranging from 25 to 100 µg·ml^{-1}. Their inhibition percentages are 47.23% to 59.34% and 49.12% to 61.47%, respectively, where the reference compound is similar to the potential of *P. vettiveroides* CNPs (Figure 10).

3.3.4 Effect of *P. vettiveroides* CNPs on superoxide anion radical scavenging assay

The *P. vettiveroides* CNPs inhibit the synthesis of blue formazan in a dosage-dependent manner (Figure 11). *P. vettiveroides* CNPs, from 25 to 100 µg·ml^{-1} of the fraction of inhibitory concentration, rises by the dose from 35.66% to 47.91%. At 25 to 100 µg·ml^{-1} with 47.42% to 61.34%, the inhibitory concentrations of the BHT and the sample derivative are virtually comparable. According to these findings, *P. vettiveroides* CNPs possess a strong superoxide radical scavenging capability.

3.3.5 Effect of *P. vettiveroides* CNPs on H_2O_2 radical scavenging assay

The *P. vettiveroides* CNPs has the capacity to scavenge H_2O_2 radicals in a dosage-dependent manner (Figure 12). The BHT has a somewhat higher degree of inhibition (46–60%) than the sample derivative, used to compare the *P. vettiveroides* CNPs. When the dose is increased from 25 to 100 µg·ml^{-1}, the *P. vettiveroides* CNPs have a percentage inhibitory concentration of 39–49%.

3.4 Anticancer activity

Concentrations of *P. vettiveroides* CNPs (25, 50, 75, 100, and 125 µg·ml^{-1}) were tested for their cytotoxicity against KB

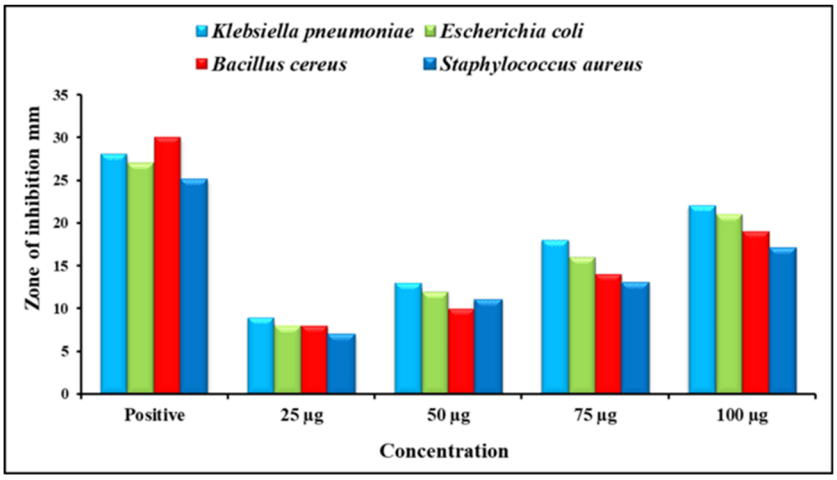

Figure 6: Graphical representation of zone of inhibition of CNPs synthesized using *P. vettiveroides* root extract.

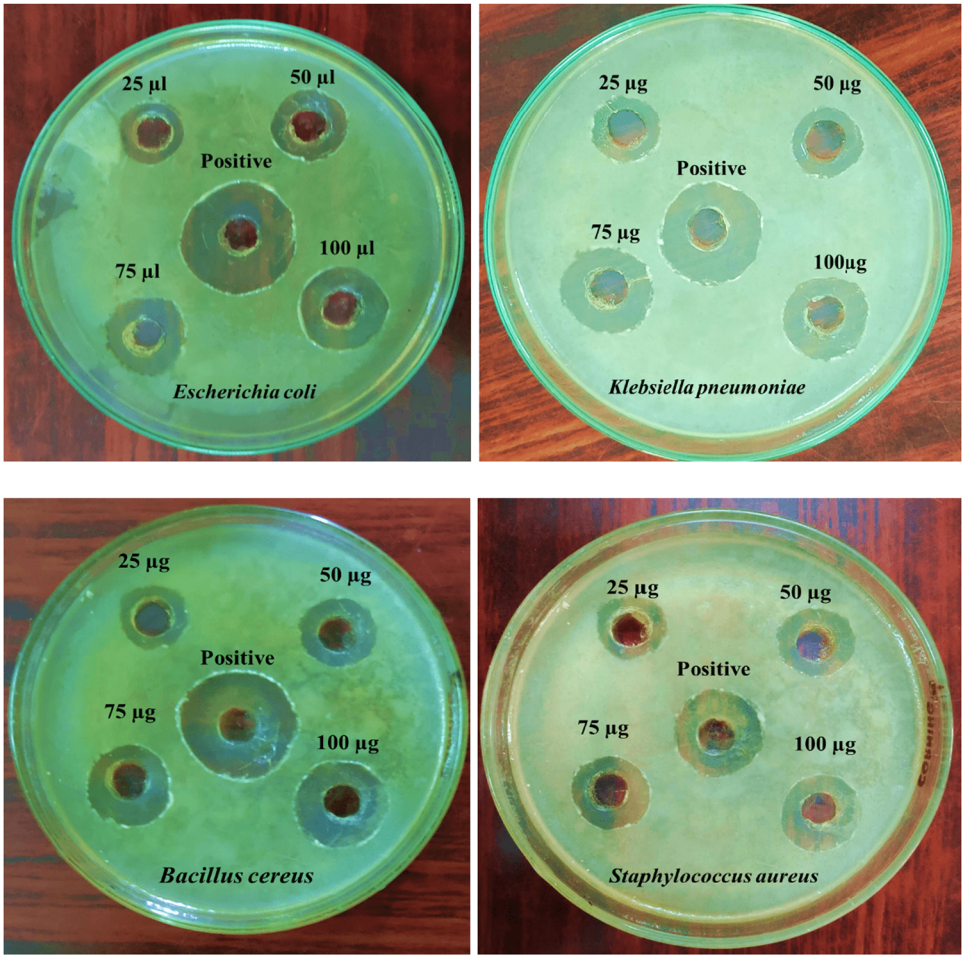

Figure 7: Antibacterial activity CNPs synthesized using *P. vettiveroides* root extract.

Table 1: Zone of inhibition of CNPs synthesized using *P. vettiveroides* root extract

Bacterial pathogens	Zone of inhibition (mm)				
	25 µg	50 µg	75 µg	100 µg	Positive
K. pneumoniae	9	13	18	22	28
E. coli	8	12	16	21	27
B. cereus	8	10	14	19	30
S. aureus	7	11	13	17	25

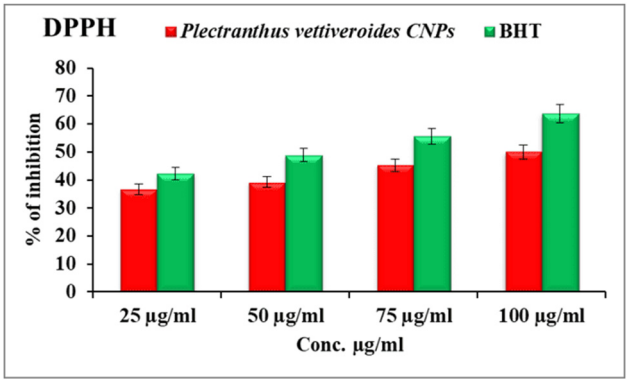

Figure 8: Effect of *P. vettiveroides* CNPs on DPPH assay.

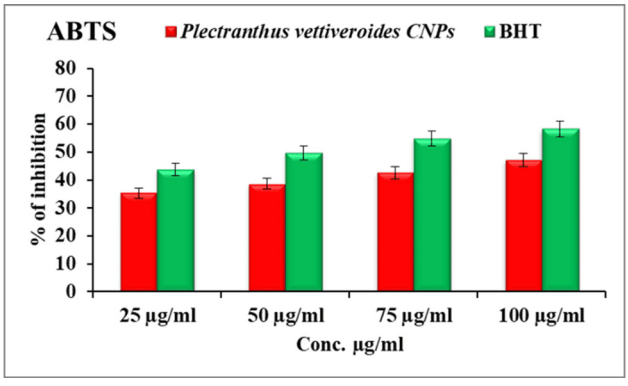

Figure 9: Effect of *P. vettiveroides* CNPs on ABTS assay.

oral cancer cells. A microscope was used to check on the growth of the cells. Under the microscope, the images of KB cells treated with *P. vettiveroides* CNPs showed cell shrinkage and condensed and shattered nuclei (Figure 13).

Lesser concentrations of *P. vettiveroides* CNPs did not cause noticeable morphological alterations. As shown in Figure 14, the substance-induced cytotoxicity in KB oral cancer cells is concentration dependent. The half-inhibitory concentration (IC50) for *P. vettiveroides* CNPs was determined to be 74 µg·ml^{-1}.

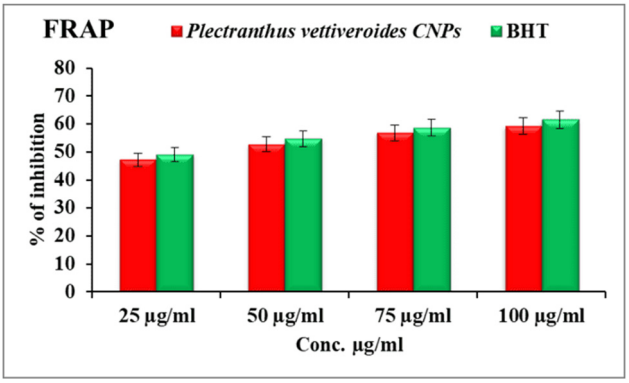

Figure 10: Effect of *P. vettiveroides* CNPs on FRAP assay.

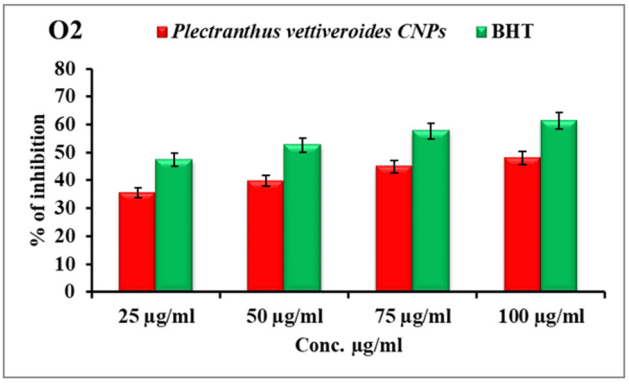

Figure 11: Effect of *P. vettiveroides* CNPs on superoxide anions.

4 Discussion

CNPs have been synthesized using a variety of different methods. When selecting a suitable preparation method, aspects such as the stability and safety of CNPs should be considered in addition to their particle size [20]. For the production of CNPs in this work, the root extract

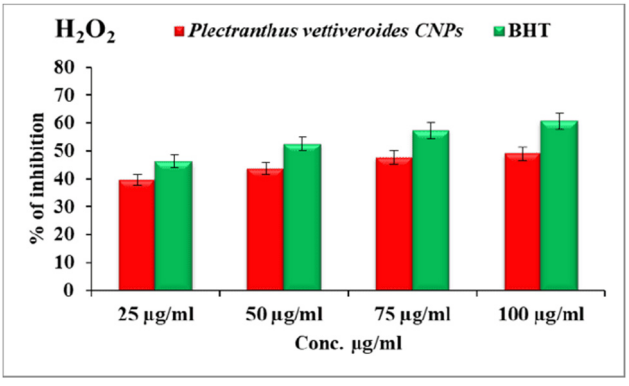

Figure 12: Effect of *P. vettiveroides* CNPs on H_2O_2.

from *P. vettiveroides* was used. The synthesis of CNPs using bioactive compounds from plant root extracts involves a stabilization mechanism. Phytochemicals present in the extracts, notably secondary metabolites, serve as stabilizers, preventing NP agglomeration by forming a capping layer on the particle surface [21]. This green synthesis method offers advantages over chemical and physical approaches by using eco-friendly sources, reducing toxic by-products, and offering a sustainable pathway for NP production. The presence of secondary metabolites facilitates the formation of green NPs, highlighting the potential of plant-derived compounds in advancing nanomaterial synthesis [22].

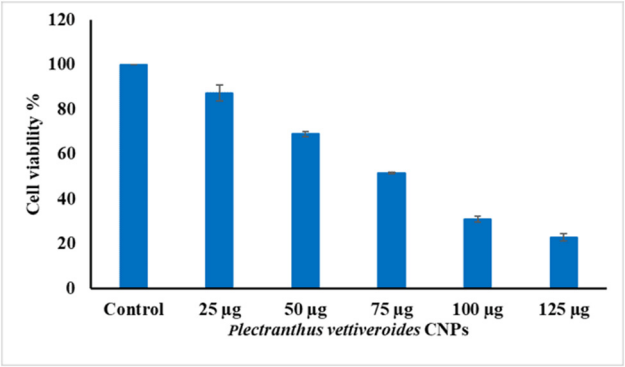

Figure 14: Effect of *P. vettiveroides* CNPs on the viability of KB cells determined by MTT assay.

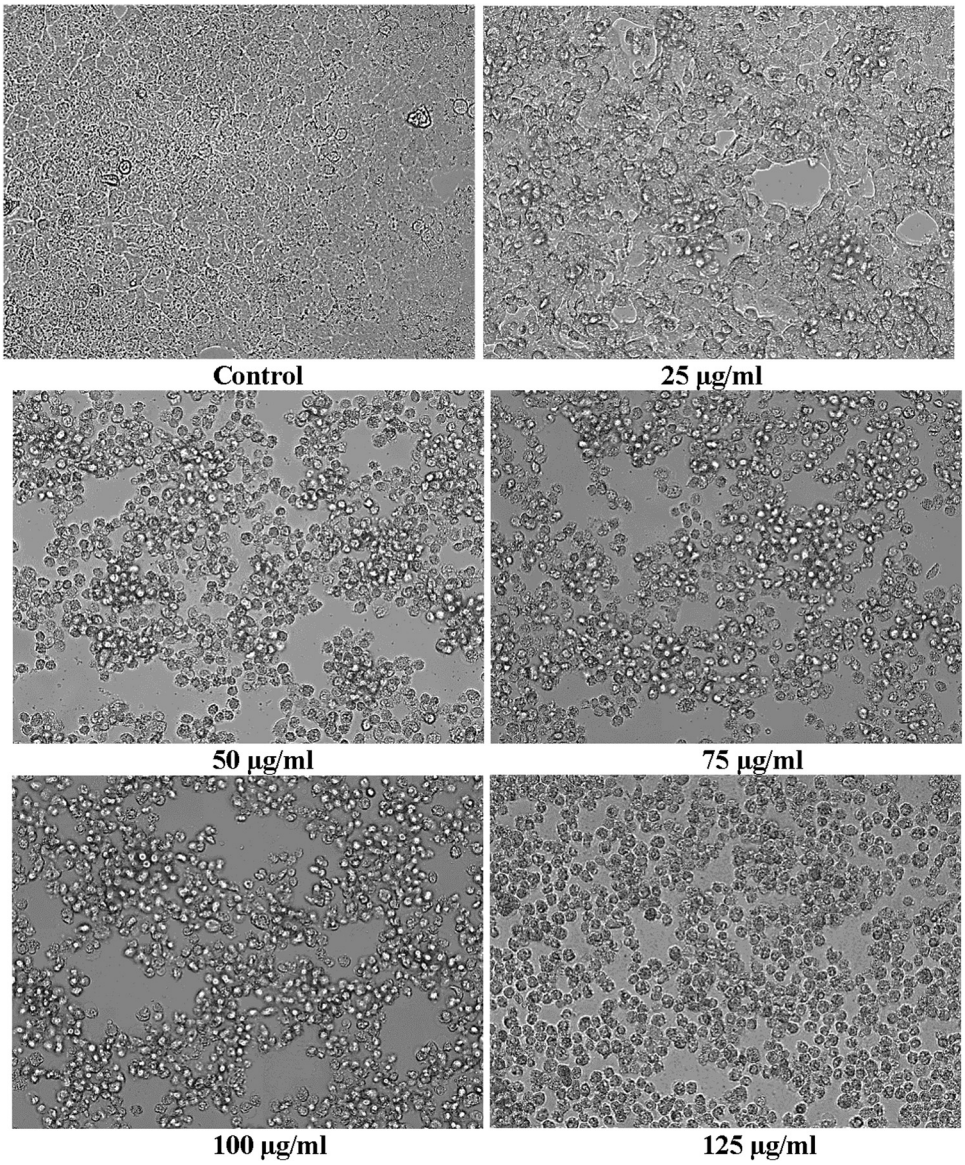

Figure 13: Morphological changes of KB cells treated with various concentrations of *P. vettiveroides* CNPs.

A main characterization test based on UV/vis spectra was used to ensure the development of the NPs. The present absorption peak wavelength was 253 nm, consistent with that previously reported in the UV region at 285 and 320 nm [23]. The CNP biopolymer's strong intensity suggests that CNPs were successfully synthesized using photosynthesis [24]. The minor peak at 645 cm^{-1} in the FTIR spectrum is the wiggling of the saccharide structure of chitosan [25]. The structural integrity of chitosan during phytoconversion into CNPs is particularly emphasized by FTIR analysis. The NPs in CNPs are well dispersed in the SEM image and are entangled to create a highly exposed surface area, which makes the CNPs ideal for adsorption [26]. Most of the CNPs made from chitosan were spherical, similar to the existing phytosynthesis of CNPs, and only a small number had an oval-pleated or rod-shaped structure [27–29].

CNPs exhibited an antibacterial activity against *K. pneumoniae* and *E. coli* [30]. The origin of CNPs' antibacterial effect may be due to the penetration and disintegration of the membrane by smaller-sized NPs, resulting in cell lysis [31]. Another theory for the mechanism behind the bactericidal action of CNPs is the release of H_2O_2 from their surface. The amount of chitosan's surface area is crucial for the production of H_2O_2, which damages the bacteria by penetrating their cell membrane [32]. The *P. vettiveroides* root extracts demonstrated a potential bactericidal activity against the tested bacteria, which could be helpful for biomedical applications. It also contains terpenoids, alkaloids, tannins, flavonoids, carbohydrates, saponins, sterols, amino acids, and proteins. CNPs tend to exhibit greater efficacy against −ve bacteria due to differences in cell wall structure. −ve bacteria have an outer lipid membrane that is less dense and provides a weaker barrier, allowing CNPs to more easily penetrate and disrupt the membrane integrity. In contrast, +ve bacteria possess a thicker peptidoglycan layer, which can hinder the penetration of CNPs, reducing their antibacterial effect. This difference in efficacy highlights the importance of considering bacterial cell wall composition when designing chitosan-based antimicrobial strategies [33,34].

Numerous ailments, including cancer and cardiovascular disease, are made worse by the generation of free radicals. Antioxidant activity can be evaluated using the well-known DPPH• free radical scavenging activity. The *P. vettiveroides* CNPs convert a violet DPPH solution to a yellow product, diphenyl picryl hydrazine, in the DPPH assay, in a dosage-dependent manner. Due to its short analytical time, this method has frequently been used to forecast the antioxidant activity of diverse substances. Since antioxidants tend to donate hydrogen, they are hypothesized to impact DPPH [35].

The $ABTS^{\cdot+}$ test can be used to evaluate antioxidant activity indirectly. The ABTS radical undergoes a strong reaction with phenolics, an H-atom donor, which creates an $ABTS^{\cdot+}$. The $ABTS^{\cdot+}$ is generally stable without phenolics [36]. The effectiveness of the antioxidants to specifically scavenge $ABTS^{\cdot+}$ is evaluated using the ABTS test and compared to BHT. It is well known that plant phenolics are potent antioxidants [37]. The observed antioxidant activity may be due to phenolic antioxidants in *P. vettiveroides* CNPs. Their capacity to operate as an antioxidant and a neutralizer of reactive species is influenced by the location of their hydroxyl atoms, the structure of phenolic compounds, and other characteristics.

The FRAP assay measures an antioxidant capacity to convert a ferric tripyridyltriazine (Fe^{3+}–TPTZ) complex into a Fe^{2+}–TPTZ complex. Reducers are substances that provide one hydrogen atom to the chain-breaking reaction of free radicals [38]. The absorbance of *P. vettiveroides* CNP increases as the concentration of the Fe^{2+}–TPTZ combination increases. The *P. vettiveroides* CNPs improved ferric reducing capacity with increasing concentration, similar to traditional antioxidants.

Superoxide, a radical with oxygen at its center, is selectively reactive. Although superoxide has a low chemical reactivity and is a very inert oxidant, it can create more hazardous species, such as singlet oxygen and hydroxyl radicals, which lead to lipid peroxidation [39]. Some enzyme systems produce these species. Superoxide anions are consequently precursors to active free radicals that can harm tissue when interacting with biological macromolecules. Superoxide anions are produced by the riboflavin/methionine/illuminate system from dissolved oxygen, reducing NBT in this system. This method produces the blue formazan, spectrophotometrically detected at 560 nm when the superoxide anion lowers the yellow dye (NBT^{2+}). The *P. vettiveroides* CNPs can stop the growth of blue formazan.

Both biological systems and beverages high in polyphenols can produce H_2O_2 when physiological conditions are met [40]. Superoxide dismutase is one of many oxidizing enzymes that can generate H_2O_2 in living things. It can pass through membranes and oxidize various things gradually. H_2O_2 is known to cause damage and *in vitro* cell death [41]. This radical can link DNA nucleotides, breaking the strand. H_2O_2 can interfere with various biological energy-producing activities [42].

NP toxicity is significantly affected by particle size and dose [43,44]. Several mechanisms allow NPs to enter cancer cells, including macro-pinocytotic uptake, clathrin-mediated transport, and caveolae-dependent endocytosis [45,46]. Once within the cell, hematite NPs can directly interact with NADPH oxidases from the plasma membrane and

mitochondria to produce superoxide anion [47,48]. This causes pro-inflammatory effects and cytotoxicity by activating redox-sensitive signaling cascades [49,50].

P. vettiveroides CNPs exhibit multifaceted biological activities. As antimicrobial agents, they inhibit microbial growth by disrupting cell membranes. Their antioxidant potential arises from scavenging free radicals, preventing oxidative stress and cellular damage. Moreover, these NPs display anticancer effects by inducing apoptosis, inhibiting cell proliferation, and modulating signaling pathways. Using these mechanisms, *P. vettiveroides* CNPs offer a promising avenue for addressing microbial infections, oxidative stress-related disorders, and cancer, showcasing their versatile therapeutic potential.

5 Conclusion

CNPs were synthesized using a biogenic method and a methanolic extract from *P. vettiveroides* root. A UV/vis spectroscopic investigation found a band at 234 nm that proved that CNPs were synthesized. SEM analysis shows that the synthesized CNPs have the shape of a sphere. Based on the results of this study, the synthesized *P. vettiveroides* CNPs have a wide range of antibacterial, antioxidant, and anticancer properties. The $DPPH^{\bullet}$, $ABTS^{\bullet+}$, FRAP, $O2^{\bullet}$, and H_2O_2 scavenging assays showed that the CNPs from *P. vettiveroides* had an antioxidant activity. At 100 $\mu g \cdot ml^{-1}$, *P. vettiveroides* CNPs had the best antioxidant activity of the three doses because they could eliminate the free radicals. At all doses tested, *K. pneumonia*, *E. coli*, *B. cereus*, and *S. aureus* were killed by *P. vettiveroides* CNPs. At 100 $\mu g \cdot ml^{-1}$, *P. vettiveroides* CNPs had the most significant effect against pathogens. The right amount of *P. vettiveroides* CNPs to fight free radicals and infections was 100 $\mu g \cdot ml^{-1}$. *P. vettiveroides* CNPs killed KB oral cancer cells in a way that depended on their concentration. Future directions might involve optimizing biogenic synthesis processes, enhancing scalability, and developing applications across various industries, aligning with eco-friendly practices. Before *P. vettiveroides* CNPs can be used in clinical use, more studies must be carried out on their antioxidant effects on living organisms.

Funding information: The authors state no funding was involved in this study.

Author contributions: Kamalesh Balakumar Venkatesan and Saravanan Alamelu – methodology and formal analysis, Sivamathi Rathna Priya – data curation, Nivedha Jayaseelan – writing-original draft preparation, Sathish-Kumar Kamaraj – writing-review and editing, Manoj Kumar Srinivasan – supervision, Mohammed Ali Alshehri, Chellasamy Panneerselvam – funding acquisition and supervision, Ahmed Saif – project administration, Selvendiran Periyasamy – characterization.

Conflict of interest: Authors state no conflict of interest.

Data availability statement: The datasets generated during and/or analysed during the current study are available from the corresponding author on reasonable request.

References

[1] Bulmer C, Margaritis A, Xenocostas A. Production and characterization of novel chitosan nanoparticles for controlled release of rHu-Erythropoietin. Biochemical Eng J. 2012 Oct;68:61–9.
[2] Rezazadeh NH, Buazar F, Matroodi S. Synergistic effects of combinatorial chitosan and polyphenol biomolecules on enhanced antibacterial activity of biofunctionalized silver nanoparticles. Sci Rep. 2020 Nov;10(1):19615.
[3] Zhao LM, Shi LE, Zhang ZL, Chen JM, Shi DD, Yang J, et al. Preparation and application of chitosan nanoparticles and nanofibers. Braz J Chem Eng. 2011;28:353–62.
[4] Su J, Zhang J, Liu L, Huang Y, Mason RP. Exploring feasibility of multicolored CdTe quantum dots for in vitro and in vivo fluorescent imaging. J Nanosci Nanotechnol. 2008 Mar;8(3):1174–7.
[5] Ahmad SI, Ahmad R, Khan MS, Kant R, Shahid S, Gautam L, et al. Chitin and its derivatives: Structural properties and biomedical applications. Int J Biol Macromolecules. 2020 Dec;164:526–39.
[6] Maraveas C. Production of sustainable and biodegradable polymers from agricultural waste. Polymers. 2020 May;12(5):1127.
[7] Tara N, Siddiqui SI, Rathi G, Chaudhry SA, Asiri AM. Nano-engineered adsorbent for the removal of dyes from water: A review. Curr Anal Chem. 2020 Feb;16(1):14–40.
[8] Calvo P, Remunan-Lopez C, Vila-Jato JL, Alonso MJ. Novel hydrophilic chitosan-polyethylene oxide nanoparticles as protein carriers. J Appl Polym Sci. 1997 Jan;63(1):125–32.
[9] Dyer AM, Hinchcliffe M, Watts P, Castile J, Jabbal-Gill I, Nankervis R, Smith A, Illum L. Nasal delivery of insulin using novel chitosan based formulations: a comparative study in two animal models between simple chitosan formulations and chitosan nanoparticles. Pharm Res. 2002 Jul;19:998–1008.
[10] Sailaja GR, Sriramavaratharajan V, Murugan R, Mallavarapu GR, Chellappan DR. Vasorelaxant property of Plectranthus vettiveroides root essential oil and its possible mechanism. J Ethnopharmacology. 2021 Jun 28;274:114048.
[11] Meireles D, Gomes J, Lopes L, Hinzmann M, Machado J. A review of properties, nutritional and pharmaceutical applications of Moringa oleifera: integrative approach on conventional and traditional Asian medicine. Adv Traditional Med. 2020 Dec;20(4):495–515.
[12] Abd-Ellatif S, Ibrahim AA, Safhi FA, Abdel Razik ES, Kabeil SS, Aloufi S, et al. Green synthesized of Thymus vulgaris chitosan nanoparticles induce relative WRKY-genes expression in Solanum

lycopersicum against Fusarium solani, the causal agent of root rot disease. Plants. 2022 Nov;11(22):3129.
[13] León-Buitimea A, Garza-Cárdenas CR, Garza-Cervantes JA, Lerma-Escalera JA, Morones-Ramírez JR. The demand for new antibiotics: antimicrobial peptides, nanoparticles, and combinatorial therapies as future strategies in antibacterial agent design. Front Microbiology. 2020;11:1669.
[14] Brand-Williams W, Cuvelier ME, Berset C. Antioxidative activity of phenolic composition of commercial extracts of sage and rosemary. Lwt. 1995;28:25–30.
[15] Re R, Pellegrini N, Proteggente A, Pannala A, Yang M, Rice-Evans C. Antioxidant activity applying an improved ABTS radical cation decolorization assay. Free Radic Biol Med. 1999 May;26(9–10):1231–7.
[16] Benzie IF, Strain JJ. Ferric reducing/antioxidant power assay: direct measure of total antioxidant activity of biological fluids and modified version for simultaneous measurement of total antioxidant power and ascorbic acid concentration. Meth Enzymol. 1999;299:15–27.
[17] Liu D, Diorio J, Tannenbaum B, Caldji C, Francis D, Freedman A, et al. Maternal care, hippocampal glucocorticoid receptors, and hypothalamic-pituitary-adrenal responses to stress. Science. 1997 Sep;277(5332):1659–62.
[18] Nabavi SM, Ebrahimzadeh MA, Nabavi SF, Fazelian M, Eslami B. In vitro antioxidant and free radical scavenging activity of Diospyros lotus and Pyrus boissieriana growing in Iran. Pharmacognosy Mag. 2009 Apr;5(18):122–6.
[19] Nair RS, Morris A, Billa N, Leong CO. An evaluation of curcumin-encapsulated chitosan nanoparticles for transdermal delivery. Aaps Pharmscitech. 2019 Feb;20:1–3.
[20] Bozkir A, Saka OM. Chitosan nanoparticles for plasmid DNA delivery: effect of chitosan molecular structure on formulation and release characteristics. Drug Delivery. 2004 Jan;11(2):107–12.
[21] Ardean C, Davidescu CM, Nemeş NS, Negrea A, Ciopec M, Duteanu N, et al. Factors influencing the antibacterial activity of chitosan and chitosan modified by functionalization. Int J Mol Sci. 2021 Jul;22(14):7449.
[22] Hosseingholian A, Gohari SD, Feirahi F, Moammeri F, Mesbahian G, Moghaddam ZS, et al. Recent advances in green synthesized nanoparticles: from production to application. Materials Today. Sustainability. 2023 Aug;24:100500.
[23] Sathiyabama M, Parthasarathy R. Biological preparation of chitosan nanoparticles and its in vitro antifungal efficacy against some phytopathogenic fungi. Carbohydr Polym. 2016 Oct;151:321–5.
[24] Oh JW, Chun SC, Chandrasekaran M. Preparation and in vitro characterization of chitosan nanoparticles and their broad-spectrum antifungal action compared to antibacterial activities against phytopathogens of tomato. Agronomy. 2019 Jan;9(1):21.
[25] de Lima PH, Tavares AA, de Lima Silva SM, de Moura MR, Aouada FA, Grillo R. Recent advances on nanohybrid systems constituting clay–chitosan with organic molecules–A review. Appl Clay Sci. 2022 Sep;226:106548.
[26] Vijayalakshmi K, Devi BM, Sudha PN, Venkatesan J, Anil SJ. Synthesis, characterization and applications of nanochitosan/sodium alginate/microcrystalline cellulose film. J Nanomed Nanotechnol. 2016;7(6):419.
[27] Sivakami MS, Gomathi T, Venkatesan J, Jeong HS, Kim SK, Sudha PN. Preparation and characterization of nano chitosan for treatment wastewaters. Int J Biol Macromolecules. 2013 Jun;57:204–12.
[28] Corazzari I, Nisticò R, Turci F, Faga MG, Franzoso F, Tabasso S, et al. Advanced physico-chemical characterization of chitosan by means of TGA coupled on-line with FTIR and GCMS: Thermal degradation and water adsorption capacity. Polym Degrad Stab. 2015 Feb;112:1–9.
[29] Mohammed MA, Syeda JT, Wasan KM, Wasan EK. An overview of chitosan nanoparticles and its application in non-parenteral drug delivery. Pharmaceutics. 2017 Nov;9(4):53.
[30] DeFilipps RA, Krupnick GA. The medicinal plants of Myanmar. PhytoKeys. 2018;102:1.
[31] Sirelkhatim A, Mahmud S, Seeni A, Kaus NH, Ann LC, Bakhori SK, et al. Review on zinc oxide nanoparticles: antibacterial activity and toxicity mechanism. Nano-micro Lett. 2015 Jul;7:219–42.
[32] Kadiyala U, Turali-Emre ES, Bahng JH, Kotov NA, VanEpps JS. Unexpected insights into antibacterial activity of zinc oxide nanoparticles against methicillin resistant Staphylococcus aureus (MRSA). Nanoscale. 2018;10(10):4927–39.
[33] Gadkari RR, Suwalka S, Yogi MR, Ali W, Das A, Alagirusamy R. Green synthesis of chitosan-cinnamaldehyde cross-linked nanoparticles: Characterization and antibacterial activity. Carbohydr Polym. 2019 Dec;226:115298.
[34] Yan D, Li Y, Liu Y, Li N, Zhang X, Yan C. Antimicrobial properties of chitosan and chitosan derivatives in the treatment of enteric infections. Molecules. 2021 Nov;26(23):7136.
[35] Kedare SB, Singh RP. Genesis and development of DPPH method of antioxidant assay. J food Sci Technol. 2011 Aug;48:412–22.
[36] Ilyasov IR, Beloborodov VL, Selivanova IA, Terekhov RP. ABTSPP decolorization assay of antioxidant capacity reaction pathways. Int J Mol Sci. 2020 Feb;21(3):1131.
[37] Cosme P, Rodríguez AB, Espino J, Garrido M. Plant phenolics: Bioavailability as a key determinant of their potential health-promoting applications. Antioxidants. 2020 Dec;9(12):1263.
[38] Nivedha J, Kanimozhi K, Olikkavi S, Vidhyasagar T, Vijayakumar N, Uma C, et al. In vitro Screening for Antioxidant and Antimicrobial Properties of 3, 5-Bis (E-thienylmethylene) piperidin-4-one, a Curcumin Analogue. Pharmacognosy. Research. 2022;14(3):276–83.
[39] Collin F. Chemical basis of reactive oxygen species reactivity and involvement in neurodegenerative diseases. Int J Mol Sci. 2019 May;20(10):2407.
[40] Akagawa M, Shigemitsu T, Suyama K. Production of hydrogen peroxide by polyphenols and polyphenol-rich beverages under quasi-physiological conditions. Biosci Biotechnol Biochem. 2003 Jan;67(12):2632–40.
[41] Wang TY, Libardo MD, Angeles-Boza AM, Pellois JP. Membrane oxidation in cell delivery and cell killing applications. ACS Chem Biol. 2017 May;12(5):1170–82.
[42] Suriyaprom S, Mosoni P, Leroy S, Kaewkod T, Desvaux M, Tragoolpua Y. Antioxidants of fruit extracts as antimicrobial agents against pathogenic bacteria. Antioxidants. 2022 Mar;11(3):602.
[43] Freyria FS, Bonelli B, Tomatis M, Ghiazza M, Gazzano E, Ghigo D, et al. Hematite nanoparticles larger than 90 nm show no sign of toxicity in terms of lactate dehydrogenase release, nitric oxide generation, apoptosis, and comet assay in murine alveolar macrophages and human lung epithelial cells. Chem Res Toxicol. 2012 Apr;25(4):850–61.
[44] Wahab R, Khan F, Al-Khedhairy AA. Hematite iron oxide nanoparticles: apoptosis of myoblast cancer cells and their arithmetical assessment. RSC Adv. 2018;8(44):24750–9.

[45] Stearns RC, Paulauskis JD, Godleski JJ. Endocytosis of ultrafine particles by A549 cells. Am J respiratory Cell Mol Biol. 2001 Feb;24(2):108–15.
[46] Shukla R, Bansal V, Chaudhary M, Basu A, Bhonde RR, Sastry M. Biocompatibility of gold nanoparticles and their endocytotic fate inside the cellular compartment: a microscopic overview. Langmuir. 2005 Nov;21(23):10644–54.
[47] Patil RM, Thorat ND, Shete PB, Bedge PA, Gavde S, Joshi MG, et al. Comprehensive cytotoxicity studies of superparamagnetic iron oxide nanoparticles. Biochem Biophys Rep. 2018 Mar;13:63–72.
[48] Sangaiya P, Jayaprakash R. A review on iron oxide nanoparticles and their biomedical applications. J Superconductivity Nov Magnetism. 2018 Nov;31:3397–413.
[49] Li N, Hao M, Phalen RF, Hinds WC, Nel AE. Particulate air pollutants and asthma: a paradigm for the role of oxidative stress in PM-induced adverse health effects. Clin Immunol. 2003 Dec;109(3):250–65.
[50] Jeng HA, Swanson J. Toxicity of metal oxide nanoparticles in mammalian cells. J Environ Sci Health Part A. 2006 Dec;41(12):2699–711.